

FLARE: A DataFlow-Aware and ScaLable HardwaRE Architecture for Neural-Hybrid Scientific Lossy Compression

Wenqi Jia*
UT Arlington
Arlington, TX, USA

Ying Huang*
UT Arlington
Arlington, TX, USA

Jian Xu*
UT Arlington
Arlington, TX, USA

Zhewen Hu
Texas A&M University
College Station, TX, USA

Sian Jin
Temple University
Philadelphia, PA, USA

Jiannan Tian
University of Kentucky
Lexington, KY, USA

Yuede Ji
UT Arlington
Arlington, TX, USA

Miao Yin[†]
UT Arlington
Arlington, TX, USA

Abstract

Scientific simulation leveraging high-performance computing (HPC) systems is crucial for modeling complex systems and phenomena in fields such as astrophysics, climate science, and fluid dynamics, generating massive datasets that often reach petabyte to exabyte scales. However, managing these vast data volumes introduces significant I/O and network bottlenecks, limiting practical performance and scalability. While cutting-edge lossy compression frameworks powered by deep neural networks (DNNs) have demonstrated superior compression ratios by capturing complex data correlations, their integration into HPC workflows poses substantial challenges due to the hybrid non-neural and neural computation patterns, causing excessive memory access overhead, large sequential stalls, and limited adaptability to varying data sizes and workloads in existing hardware platforms. To overcome these challenges and push the limit of high-performance scientific computing, we for the first time propose FLARE, a dataflow-aware and scalable hardware architecture for neural-hybrid scientific lossy compression. FLARE minimizes off-chip data access, reduces bubble overhead through efficient dataflow, and adopts a modular design that provides both scalability and flexibility, significantly enhancing throughput and energy efficiency on modern HPC systems. Particularly, the proposed FLARE achieves runtime speedups ranging from 3.50× to 96.07×, and energy efficiency improvements ranging from 24.51× to 520.68×, across various datasets and hardware platforms.

Keywords

Dataflow Optimization, Scalable Architecture, Lossy Compression, High-Performance Scientific Computing

1 Introduction

Scientific simulation powered by high-performance computing (HPC) enables researchers to model complex natural systems at unprecedented scale and fidelity. It allows for accurate predictions and insights in fields like climate science, physics, and biology, where real-world experimentation is costly, slow, or impossible [3, 7, 33]. For example, cosmological simulations based on Dark Matter Evolution and Self-Gravity Equations [1, 34] leverage HPC to model the Lyman- α forest, baryonic matter distribution, and thermodynamics of the intergalactic medium (IGM), offering more profound insights into early-universe astrophysics [27, 30]. However, to accelerate scientific discovery and inform critical decisions, these applications

routinely generate petabyte- to exabyte-scale data as model complexities grow. For instance, the CMIP climate project [29] produced 2.5 PB of data, and cutting-edge fluid dynamics [13] runs can yield hundreds of terabytes per simulation. Storing and accessing such massive data on existing HPC systems can overwhelm shared I/O resources, degrading disk performance and impacting other users' read/write operations [2, 15, 32]. Worse yet, transferring these data across systems or storage tiers can saturate network bandwidth, leading to contention and delays [4, 14]. These I/O and communication bottlenecks highlight the need to reduce source data volume. Efficient data compression has thus become crucial for managing and scaling with the realities of modern scientific data generation on HPC systems.

Early efforts in scientific data compression focused on lossless techniques [5, 8, 21, 40], which typically achieve limited ratios (1×–3×) on scientific data [39]. In contrast, lossy compression methods [6, 18–20, 24, 35, 36, 38] offer much higher ratios – for example, up to 436× with SZ [6] – while allowing slight fidelity loss within user-defined error tolerances, which indeed alleviates storage bottlenecks and reduces bandwidth. Among its core components, predictors, such as curve fitting [6] and spline interpolation [16], play a crucial role in exploiting local data correlations. However, these methods use *pre-determined*, *closed-form* approximation, which often fails to capture complex or irregular features in scientific data. As a result, they may overlook latent correlations and ultimately degrade compression efficiency. Deep neural networks (DNNs), known as powerful predictors [9], have shown strong potential in lossy compression [11, 12, 17, 22, 23, 26]. By enhancing hand-crafted predictors, DNNs better handle irregular data features and, therefore, improve compression efficacy. As a result, combining traditional compressors with learning-based models has become a promising trend for high-ratio, error-bounded scientific data reduction.

Neural-hybrid lossy compression integrating DNNs offers impressive compression ratios and reconstruction quality, but introduces significant challenges in computational cost and data movement across multiple general-purpose hardware systems. **1 CPU-only** systems generally struggle to support the high data volumes required for efficient processing: the typical throughput of CPU-based compressors is at an order of magnitude of 10^{-1} gigabytes/sec [25], far below the data rates generated by modern simulators and sensors [37]. Furthermore, the limited *parallelism* and *concurrency* [28] cap the neural capabilities, such as convolutions and matrix multiplications. **2 GPU-only** systems, equipped

*Equal contributions. [†]Corresponding author. Email: miao.yin@uta.edu.

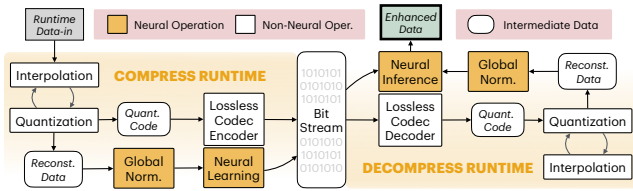


Figure 1: Overview of the state-of-the-art neural-hybrid lossy compression method, NeurLZ. "Global Norm." denotes the global normalization step.

with thousands of parallel cores, can efficiently execute neural operations and demonstrate throughput improvements ranging from $10\times$ to $100\times$ over CPUs. However, GPU efficiency is often compromised by non-neural components, such as interpolation and lossless encoding, which are sequential or control-flow intensive, leading to underutilization of GPU resources. Additionally, frequent kernel launches and the memory-bound nature of non-neural operations exacerbate this inefficiency. ³ To address the limitations of single hardware platforms, CPU-GPU pipelines have been proposed. However, these hybrid systems suffer from significant data transfer overheads via PCIe, especially when neural inference is performed on the GPU and subsequent data reconstruction occurs on the CPU. This overhead leads to considerable performance degradation, as the benefits of GPU acceleration are often negated by the latency induced by data movement. Consequently, hybrid architectures often fail to meet performance expectations, which has sometimes prompted the design of customized hardware platforms [10].

While an application-specific ASIC appears to be a natural solution to the limitations of general-purpose processors, a naive implementation of neural-hybrid lossy compression faces significant challenges. First, the level-wise predictor introduces a memory-bound bottleneck due to irregular access patterns and extensive intermediate data that saturate on-chip buffers and exert excessive pressure on off-chip bandwidth. Second, the absence of inter-stage pipelining leads to severe idle cycles, as each module – predictor, neural network, and lossless codec – must wait for its predecessor to finish before commencing execution. Third, fixed-function datapaths hinder scalability, making it difficult to adapt to varying data sizes and workloads without costly hardware redesign.

To overcome the aforementioned limitations and enhance the runtime energy efficiency of neural-hybrid lossy compression, we propose FLARE, a dataflow-aware and scalable hardware architecture that delivers three key innovations:

- **Look-ahead computation ordering**, which strategically reorders prediction operations to reduce intermediate buffer usage, enabling efficient on-chip storage and minimizing costly off-chip DRAM accesses through improved data locality.
- **Slice-wise normalization with operator fusion**, which replaces memory-intensive global normalization with a localized, slice-based approach to enable fine-grained pipelining, while fusing normalization into the convolution operator to eliminate redundant memory movement.
- **Dataflow-aware scalable design**, which implements a hybrid pipelined-parallel execution model that minimizes

inter-stage communication overhead and dynamically adapts to varying data sizes and workloads without requiring hardware reconfiguration.

To the best of our knowledge, FLARE is the first scalable hardware architecture for neural-hybrid scientific lossy compression. Experimental results show that FLARE achieves substantial performance improvements, with runtime speedups ranging from $3.50\times$ to $96.07\times$ and energy efficiency gains between $24.51\times$ and $520.68\times$ across diverse datasets and platforms.

2 Background and Motivation

2.1 Neural-Hybrid Lossy Compression

The state-of-the-art neural-hybrid lossy compressor, NeurLZ [12], adopts a hybrid design that preserves compatibility with conventional compression pipelines while selectively integrating neural modules to enhance reconstruction accuracy, based on the SZ3 [19] algorithm. As illustrated in Figure 1, NeurLZ integrates conventional non-neural components (i.e., interpolation-based prediction, quantization, and lossless encoding/decoding), with lightweight neural operators that are trained online to enhance prediction accuracy.

During compression, the input data is initially processed by a conventional lossy compressor that employs level-wise, block-based iterative interpolation, as illustrated in Figure 3. At each level, the reconstructed data from the previous level are partitioned into fixed-size blocks, where an interpolation module predicts new data values based on neighboring values generated earlier along each data dimension. The resulting prediction error, defined as the difference between the original and interpolated values, can be significant and is subsequently quantized within a user-specified error bound. This quantization step produces two outputs: (1) the quantization code, which is passed to a lossless compressor for entropy encoding and forms part of the final compressed bitstream, and (2) the reconstructed value, derived from the interpolation prediction and the quantization code, which serves as the reference for predicting data in subsequent levels, thereby preserving continuity and enhancing prediction accuracy. After all reconstructed data are generated by the conventional compressor, they are globally normalized and passed to a lightweight neural network module for online training. This neural module extracts additional features that are appended to the output stream, enriching the learned representation.

The procedure operates in reverse order during decompression. It begins by decoding the quantization codes from the bitstream using a lossless decoder, followed by reconstructing each data point via iterative interpolation, leveraging previously reconstructed values as reference. After completing the full reconstruction, a global normalization step is applied, and the normalized data is further refined through a lightweight neural network whose parameters are retrieved from the bitstream to enhance final reconstruction quality.

2.2 Analysis of General Hardware

CPU and GPU are the most common general hardware, which have been widely used for various computing applications. However, those general-purpose platforms are not well-aligned with the hybrid workload of NeurLZ, which combines control- and

Table 1: CPU and GPU Specifications for Evaluation.

Platform	CPU Model	GPU Model
Plat-1	AMD EPYC 9254	NVIDIA RTX 6000 Ada
Plat-2	Intel Xeon w5-3435X	NVIDIA RTX 4090
Plat-3	Intel Core i7-5930K	NVIDIA GTX 1080 Ti

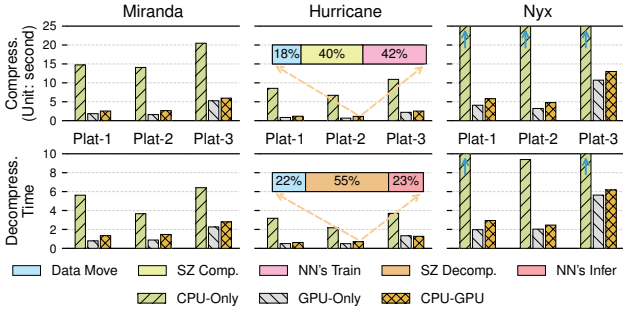


Figure 2: Processing time of three platforms across three common datasets on CPU-only, GPU-only, and CPU-GPU systems. The breakdown details the time composition of CPU-GPU on Hurricane at Plat-2.

memory-bound non-neural components with compute-intensive, parallelizable neural components. This heterogeneity leads to inefficient resource utilization and performance bottlenecks. We evaluate NeurLZ on three platforms with varying CPU and GPU capabilities (Table 1) under three configurations: (1) **CPU-only**, where both components run on the CPU, suffers from poor parallelism support for neural component and exhibits the worst runtime; (2) **GPU-only**, where both components run on the GPU with non-neural parts optimized using cuSZ [37], achieves the lowest runtime but at the cost of reduced compression ratio; and (3) **CPU-GPU**, which assigns non-neural components to the CPU and neural components to the GPU, maintains high compression performance but incurs longer runtime than GPU-only due to CPU-GPU data transfers via PCIe. For instance, the breakdown for the Hurricane dataset on Plat-2 shows that PCIe communication accounts for 18% and 22% of the total processing time for compression and decompression, respectively. Compression ratios for CPU-only, GPU-only, and CPU-GPU are 387×, 25×, and 387× on Miranda; 16,000×, 31×, and 16,000× on Nyx; and 20×, 16×, and 20× on Hurricane, respectively. Runtime comparisons are shown in Figure 2.

2.3 Challenges for Customized Hardware

Customized hardware platforms can be tailored to exploit the inherent characteristics of NeurLZ, offering notable advantages in performance and energy efficiency. However, naive implementations fall short due to three key challenges.

1 The algorithm is fundamentally **memory bounded**, driven by three key sources of repeated and irregular memory access. **First**, the level-wise block-based interpolation repeatedly accesses the same reconstructed data across levels. At each level, reconstructed data is fetched from off-chip memory and partitioned into multiple

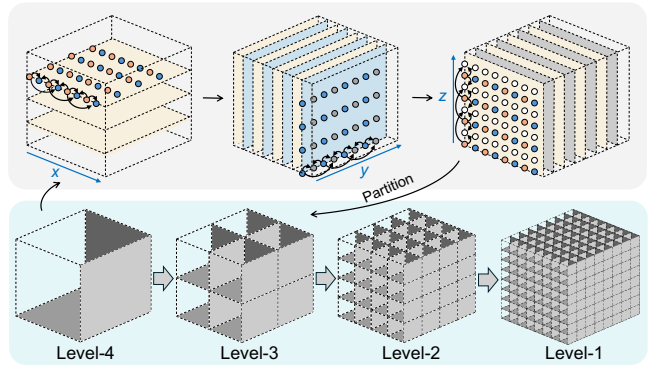


Figure 3: Level-wise, block-based interpolation. The upper part illustrates interpolation in a single block.

fixed-size blocks, within which new reconstructed data and quantized errors are computed. These outputs are written back to off-chip memory, and both the newly and previously reconstructed data are used as reference points in the next level, resulting in frequent and redundant memory accesses. **Second**, access irregularity arises both from the linear mapping of multidimensional scientific data into one-dimensional memory and the intrinsic non-contiguity of the interpolation process. Specifically, the stride between adjacent reconstructed points varies across levels and data dimensions (e.g., X, Y, and Z), resulting in non-sequential and discontinuous memory access. These irregular patterns cause frequent cache misses and increased off-chip traffic, degrading overall throughput. **Third**, global normalization, which prepares data for neural network input, introduces additional overhead. It requires two full-memory sweeps: one to compute the global minimum and maximum, and another to apply normalization. This step contributes substantial data movement and further exacerbates the overhead. As evidenced in Figure 2, during the decompression process for Hurricane, non-neural components, despite requiring only 0.23% of the FLOPs compared to the neural part, still consume nearly 2× latency, illustrating that memory bottlenecks dominate despite low computational demand. While on-chip SRAM can buffer intermediate data to alleviate the overhead, the required capacity becomes impractical for large-scale scientific datasets.

2 **Bubble overhead** arises due to the global normalization process, which prevents the system from maintaining a fully pipelined execution. Although partial quantized errors can be forwarded to the lossless encoder for efficient pipelining, global normalization requires access to the entire reconstructed dataset. This dependency delays the neural network, which processes data at a fine-grain two-dimensional slice level, until normalization is finished, thereby substantially reducing pipeline efficiency.

3 **Limited scalability** in fixed-function datapaths hinders efficient handling of diverse data sizes and workload characteristics. Over-provisioned designs lead to unnecessary silicon area and energy overhead, while under-provisioned ones fail to meet latency constraints. These challenges underscore the need for a more efficient, scalable, and dataflow-aware architecture to support neural-enhanced lossy compression at scale.

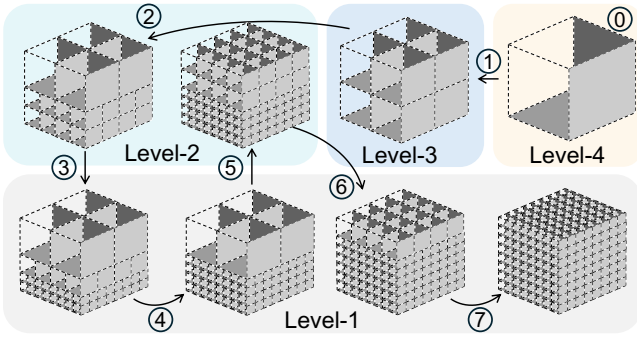


Figure 4: Proposed look-ahead computation order. Circled numbers indicate the execution steps.

3 Proposed Hardware: FLARE

3.1 Look-ahead Computation Order

To address intensive memory access challenges and mitigate costly irregular data access patterns within limited on-chip SRAM capacity, we propose a look-ahead computation order that substantially reduces SRAM requirements for intermediate results while preserving algorithmic efficiency. The core idea is to leverage data locality inherent in the level-wise block-based interpolation procedure by carefully reordering execution to maximize the reuse of reconstructed data. Since interpolation operations are inherently independent across blocks, significant data reuse opportunities exist at different processing levels. Our approach enables partial block-granularity computations to span across multiple levels, initiating execution for subsequent levels before completing the current one. Intermediate results from partially processed blocks, whose sizes are significantly reduced, can thus be buffered in SRAM, effectively avoiding expensive off-chip memory transactions. By exploiting block-wise independence and intrinsic level-wise locality, the proposed method facilitates the early reuse of partial results, substantially reducing both the memory footprint and the capacity demand on on-chip SRAM. Ultimately, once data locality at level-1 is fully exploited, these partial results are directly forwarded to downstream modules, as they are no longer needed in subsequent interpolations.

Figure 4 illustrates the proposed look-ahead strategy. At each level, only half of the newly reconstructed blocks are immediately forwarded to the next level for further processing, while the remaining half is deferred until the first half completes processing at Level-1, thus generating partial final results. For instance, the lower half of reconstructed blocks at Level-3 is processed earlier at Level-2 (step 2), whereas the upper half is processed later at step 5, after the lower half has been fully computed through Level-1. Because results from Level-1 are not needed for subsequent computations, this approach significantly reduces the SRAM capacity requirement by 3.46 \times , as depicted in Figure 5, assuming a fixed block size of $32 \times 32 \times 32$ with 32-bit values. In contrast, the original computation order requires the entire dataset to be stored in SRAM to avoid excessive off-chip memory accesses, which becomes impractical for large-scale scientific datasets.

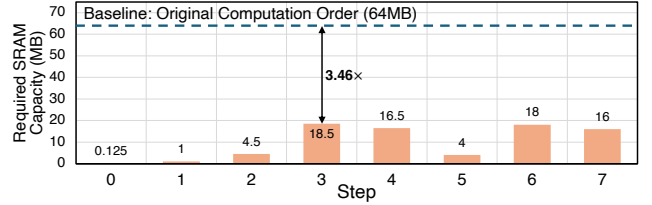


Figure 5: Reduction in SRAM capacity by the proposed computation order compared to the baseline.

Essentially, the proposed look-ahead computation order adopts a Depth-First Exploration strategy – a recursive traversal that processes data blocks in a depth-first manner, producing partial results early in the computation. Unlike the original Breadth-First Exploration approach, which fully processes all blocks at each level before proceeding to the next, our depth-first approach enables an efficient execution order that exploits data locality to eliminate redundant data accesses, minimize memory usage, and enhance overall performance. By processing blocks across levels in an out-of-order fashion, the proposed algorithm effectively manages memory resources and reduces latency, making it particularly suitable for high-performance computing applications.

3.2 Slice-wise Normalization with Operator Fusion

Global normalization in the neural component ensures each data point is appropriately scaled and centered before neural network processing, facilitating enhanced feature extraction. However, this incurs significant memory access redundancy and large bubble overhead due to repeated full-dataset memory traversals. To address this, we propose a slice-wise instance normalization technique that operates directly on two-dimensional data slices. This approach aligns with the neural network’s slice-based execution pattern, enabling a fully pipelined dataflow in a finer-grained manner. Specifically, each normalized slice can be streamed directly to the neural component on the fly, effectively eliminating the overhead associated with global normalization across the entire dataset.

Furthermore, this strategy aggressively reduces memory accesses and enhances data access efficiency by fusing the normalization operation with the convolution kernel. Specifically, we introduce two variables, max_i and min_i , to track the maximum and minimum values for the i -th slice during the prediction procedures. By embedding normalization directly into the convolution kernel, the separate read and write operations for normalized data are eliminated. For each data point $D[x, y, i]$ in the i -th slice, the normalized value is computed as:

$$D_N[x, y, i] = \frac{D[x, y, i] - min_i}{max_i - min_i} \quad (1)$$

where $D_N[x, y, i]$ denotes the normalized data. Integrating this normalization into the computation of the first convolution layer

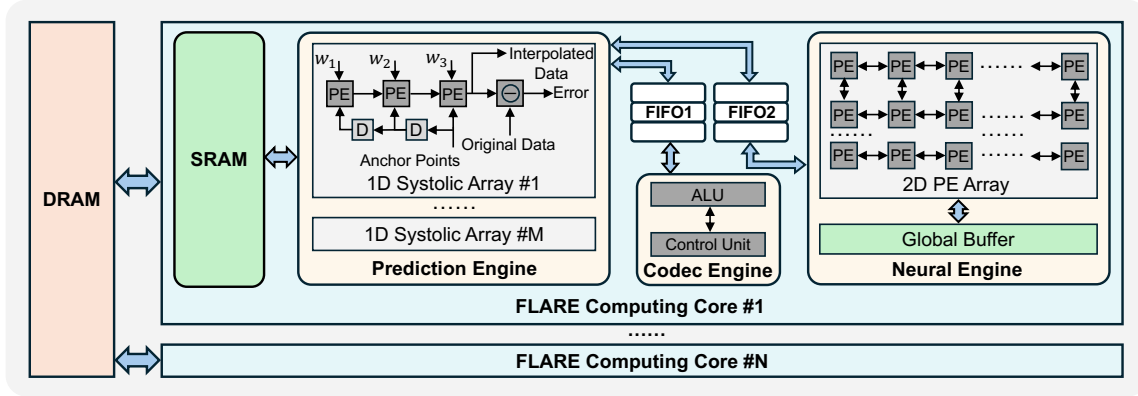


Figure 6: Architecture overview of the proposed FLARE.

yields the convolution output $O[x, y, o]$:

$$O[x, y, o] = \sum_{k_x, k_y} D_N[x + k_x, y + k_y, i] \cdot W[k_x, k_y, o] + b[o] \quad (2)$$

$$= \sum_{k_x, k_y} \frac{D[x + k_x, y + k_y, i] - \min_i}{\max_i - \min_i} \cdot W[k_x, k_y, o] + b[o] \quad (3)$$

$$= \sum_{k_x, k_y} D[x + k_x, y + k_y, i] \cdot W'[k_x, k_y, o] + b'[o] \quad (4)$$

where the updated convolution weights $W'[k_x, k_y, o]$ and $b'[o]$ incorporating normalization parameters, are computed as:

$$W'[k_x, k_y, o] = \frac{W[k_x, k_y, o]}{\max_i - \min_i} \quad (5)$$

$$b'[o] = b[o] - \sum_{k_x, k_y} \frac{\min_i}{\max_i - \min_i} \cdot W[k_x, k_y, o] \quad (6)$$

Compared to explicitly computing $D_N[x, y, i]$, updating the convolution kernel $W'[k_x, k_y, o]$ and $b'[o]$ introduces minimal additional workload due to the small size. Furthermore, the compression quality achieved by the proposed instance normalization remains comparable to that of the original global normalization, as analyzed in Section 4.1.

3.3 Dataflow-Aware and Scalable Design

The proposed look-ahead computation order and slice-wise normalization jointly enable the normalization of reconstructed data and the generation of quantized errors at a finer granularity, facilitating prediction in a slice-wise order. Hence, the prediction modules (interpolation and quantization), lossless codec module, and neural network components in the NeurLZ framework are executed together through a hybrid dataflow pattern that integrates both pipelined and parallel processing. During compression, at each time step, the prediction modules generate a batch of slices, with the batch size determined by the block size. While subsequent slices are being computed, the current batch is immediately dispatched downstream to the neural network and lossless codec module, forming a **pipelined dataflow**. Concurrently, the reconstructed slices are used by the neural network for error feature extraction, and the

lossless codec, such as an entropy encoder, processes the quantized errors. This concurrent usage establishes a **parallelized dataflow**. During decompression, the computation order is reversed. The dependency from Huffman decoding to data prediction creates a fine-grained **pipelined dataflow** across lossless decoding, prediction, and neural network inference. This hybrid execution pattern enables efficient processing at a fine granularity in both compression and decompression, thereby improving throughput and scalability.

To support an efficient hybrid dataflow and enable scalability across diverse datasets and workloads, we propose a dataflow-aware, scalable **FLARE Computing Core**, which integrates prediction (including interpolation and quantization), neural network, and lossless codec components, as depicted in Figure 6. By leveraging the hybrid dataflow, intermediate results can be stored on-chip, allowing each component to operate on the fly and significantly reducing costly off-chip data movement, thereby improving overall throughput. Meanwhile, although the micro-architectures of individual modules are carefully customized to match their distinct computational and memory access patterns for maximum efficiency, the architecture remains modular and scalable, supporting a wide range of data sizes and workload configurations without sacrificing performance.

The FLARE Computing Core consists of four primary components: (1) an on-chip *SRAM buffer*, (2) a *Prediction Engine* for processing interpolation and quantization, (3) a *Neural Engine* for neural network operations, and (4) a *Codec Engine* for lossless Huffman codec as compression encoder and decompression decoder.

The on-chip *SRAM buffer* serves as a high-bandwidth, low-latency temporary storage layer, significantly reducing the need for frequent and costly off-chip DRAM accesses. It provides fast data access to the Prediction Engine, enabling efficient pipelined execution of upstream modules.

The *Prediction Engine* comprises M one-dimensional (1D) systolic arrays, each dedicated to performing interpolation and quantization for a single data block. Each array executes matrix-vector multiplications using fixed interpolation coefficients (e.g., (w_1, w_2, w_3) in cubic interpolation). A sliding-window mechanism streams neighboring anchor points through the processing elements (PEs) in a pipelined fashion, enabling high data reuse and reducing latency.

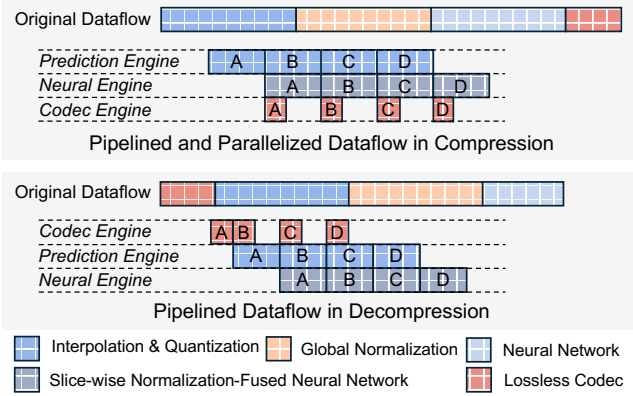


Figure 7: Illustration of compression and decompression dataflow.

Within each array, the interpolation error is computed by comparing the interpolated values with the original data. This error is then quantized, while the quantization code can be used in data reconstruction. Since each block is processed independently, the engine can simultaneously handle up to M blocks in parallel, effectively leveraging coarse-grained parallelism across blocks.

The *Neural Engine* accelerates compute-intensive neural network operations and features a two-dimensional (2D) PE array optimized for common workloads such as convolutions, matrix multiplications, and attention mechanisms. The grid-based layout enables parallel processing across multiple data streams with efficient dataflow control. To mitigate DRAM bandwidth limitations, the Neural Engine includes a dedicated global buffer for caching intermediate results locally, which reduces off-chip data movement and enables sustained throughput during training or inference.

The *Codec Engine* consists of ALU-based processing elements for control-intensive and low-compute Huffman encoding and decoding. These tasks involve intensive branch and control logic, tightly integrated with the Prediction Engine to compress or decompress quantized error values immediately.

As shown in Figure 7, during compression, outputs from the Prediction Engine are streamed slice-wise to both the Neural and Codec Engines, enabling concurrent execution and full support for the hybrid dataflow. However, due to the look-ahead computation order in the Prediction Engine, the output rate is non-uniform, with variable intervals between consecutive outputs. To manage this variability and ensure uninterrupted execution, two FIFO-based circular buffers, i.e., *FIFO1* and *FIFO2*, are introduced to temporarily store quantized errors and reconstructed data, respectively. These buffers enable efficient data staging and retrieval, maintaining a fully pipelined dataflow with minimal overhead. A similar pipeline is applied during decompression.

Meanwhile, the FLARE Computing Core architecture is designed with a modular and scalable structure, offering flexibility in two key dimensions. **Data-size scalability** allows the architecture to handle a wide range of input sizes by adjusting the parameter M , which determines the number of parallel systolic arrays in the Prediction Engine. By tuning M , the processing throughput can be aligned with the computational capabilities of the Neural Engine, ensuring

Table 2: Property of tested datasets.

Dataset	Size (GB)	Dimension	Domain
Nyx	0.5	(512, 512, 512)	Cosmology
Miranda	0.28	(256, 384, 384)	Large Turbulence
Hurricane	0.1	(100, 500, 500)	Weather

balanced execution across modules. **Workload scalability** enables concurrent processing of multiple datasets by scaling N , the number of FLARE Computing Cores. For heavy workloads, multiple cores can be instantiated in parallel to meet performance demands. This modularity allows the architecture to scale efficiently with varying data sizes and workload intensities, without requiring an architectural redesign.

4 Evaluation

4.1 Algorithm Performance Evaluation

We evaluate the proposed slice-based normalization algorithm within the NeurLZ framework, which employs a U-Net-based neural network architecture. In this evaluation, the original global normalization is replaced by the proposed slice-based method, as described in Section 3.2. Experiments are conducted on three representative scientific datasets—Nyx, Miranda, and Hurricane—spanning diverse data types and sizes, as summarized in Table 2. For fair comparison, a uniform error bound of 10^{-3} is applied across all evaluated methods, including the original SZ3, NeurLZ, and our proposed approach. Reconstruction quality is measured using Peak Signal-to-Noise Ratio (PSNR), with higher values indicating better quality.

As illustrated in Figure 8, the proposed slice-based normalization consistently outperforms the original SZ3 algorithm, achieving a substantial PSNR improvement of 6–10 dB across all datasets due to enhanced neural network training. While the initial PSNR is slightly lower than that of NeurLZ, it improves steadily with continued training. After 5–6 epochs, the PSNR becomes comparable to NeurLZ, demonstrating the effectiveness of slice-based normalization in improving reconstruction quality without compromising compression performance.

4.2 Evaluation Setup for Architecture

Hardware configuration. The evaluation is performed on a single-core configuration ($N = 1$), with an on-chip SRAM capacity of 32 MB. The Prediction Engine employs four 1D systolic arrays, enabling concurrent interpolation of four data blocks, each sized $32 \times 32 \times 32$. FIFO1 and FIFO2 are configured with capacities of 8 MB and 32 MB, respectively. The Neural Engine consists of a 128×128 2D PE array, supported by a 24 MB global buffer. A detailed summary of the architectural parameters is presented in Table 3.

Simulation and CAD tools. The high-level functional behavior of the Computing Core is initially modeled using a bit-accurate, cycle-accurate simulator. Based on this model, a corresponding RTL implementation in Verilog is developed and functionally verified through extensive simulation. The verified RTL is synthesized using Synopsys Design Compiler with a 28 nm CMOS technology library, targeting a 1 GHz clock frequency. After synthesis,

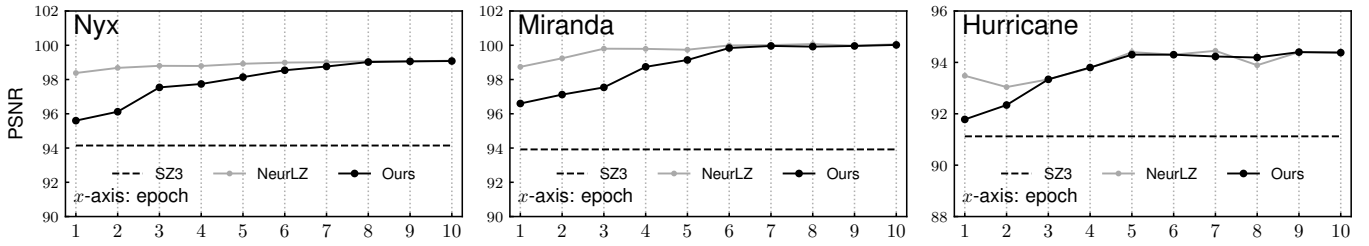


Figure 8: Algorithm performance curves of our proposed FLARE.

Table 3: Configuration of FLARE Computing Core

Component	Parameter	Value
SRAM	Capacity	32 MB
Interpolation Engine	M	4
FIFO1	Capacity	8 MB
FIFO2	Capacity	32 MB
Neural Engine	Size of 2D PE Array	128×128
	Global Buffer Size	24 MB

place-and-route is carried out using Synopsys IC Compiler, and the resulting gate-level netlist is annotated with toggle rates extracted from simulation-based switching activity, enabling accurate power estimation. We use Synopsys PrimeTime PX to evaluate both dynamic and static power consumption. The area and power of memory components are estimated separately using Cacti. To further improve performance on the customized architecture, we use TimeLoop [31] to explore intra-layer dataflow optimizations for neural network training and inference. The final synthesized results report a power of 7.38 W and a chip area of 100.07 mm^2 .

Baseline and benchmarks. To enable a fair evaluation, we adopt the same datasets and error bounds as used in the original NeurLZ paper. Specifically, the three scientific computing datasets are listed in Table 2, each with a fixed error bound of 10^{-3} . The baselines include NeurLZ implemented on three system configurations: CPU-only, GPU-only, and a CPU-GPU hybrid system. The hardware specifications for the CPU and GPU platforms are detailed in Table 1. For the GPU-only configuration, the cuSZ [37] is used to ensure fair comparison.

4.3 Evaluation Result

Compression performance. We evaluate the compression performance of the proposed FLARE across all systems and platforms using the Nyx, Miranda, and Hurricane datasets. Although our method requires additional epochs to achieve the same PSNR as NeurLZ, it still delivers significant gains in both speed and energy, due to its optimized dataflow and architectural support. As shown in Figure 9, on Nyx we observe $4.61\times-96.07\times$ runtime reduction and $31.27\times-520.68\times$ energy efficiency improvement; on Miranda, $5.75\times-81.48\times$ runtime reduction and $33.54\times-441.65\times$ energy efficiency gains; and on Hurricane, $3.50\times-68.16\times$ runtime reduction alongside $24.51\times-369.45\times$ energy efficiency improvements. These results confirm that our design not only accelerates lossy compression but also substantially lowers energy consumption.

Decompression performance. FLARE also achieves promising results in decompression. Specifically, on Nyx dataset, it delivers $4.69\times-37.96\times$ runtime speedups and $38.11\times-247.47\times$ energy efficiency improvements; on Miranda, $4.36\times-35.59\times$ runtime speedups and $35.48\times-192.89\times$ energy efficiency gains; and on Hurricane, FLARE achieves $4.90\times-37.04\times$ runtime speedups alongside $35.02\times-200.78\times$ energy efficiency improvements. These consistent gains across diverse datasets and platforms highlight the generality and scalability of our architecture for both compression and decompression processes.

4.4 Ablation Study

Scalability of the architecture. The proposed modular architecture is designed with scalability as a core principle, offering two key dimensions of flexibility: data size scalability and workload scalability.

In terms of data-size scalability, the architecture allows flexible adjustment of the number of 1D systolic arrays (M) within each FLARE Computing Core to accommodate different dataset sizes or computational intensities. By increasing M , a single core can efficiently process larger blocks or more data in parallel, thereby reducing runtime. As shown in Figure 10, we evaluate the compression and decompression runtime of the Nyx dataset by scaling M from 1 to 8. The results show a clear reduction in decompression time as M increases. However, compression speedup is less pronounced due to the fully pipelined dataflow and the compute-intensive nature of neural network training, where the Neural Engine becomes the dominant bottleneck. For example, after $M = 4$, the runtime reaches its minimum despite additional systolic arrays.

For workload scalability, the architecture supports parallel execution across multiple FLARE Computing Cores (N), each operating independently to process distinct dataset or computational task concurrently. This capability is particularly advantageous for large-scale deployments, where multiple datasets or workloads must be processed simultaneously to improve overall system throughput and reduce latency. To demonstrate this, we evaluate runtime performance while concurrently processing two Nyx datasets, one Miranda dataset, and one Hurricane dataset as we scale the number of cores from 1 to 4. As shown in Figure 10, runtime consistently decreases with additional cores. However, when scaling from $N = 3$ to $N = 4$, the simultaneous processing of two Nyx datasets becomes the dominant bottleneck, achieving performance at 1.16 seconds for compression and 0.42 seconds for decompression.

These results demonstrate that the proposed architecture effectively scales along both data size and workload dimensions. The

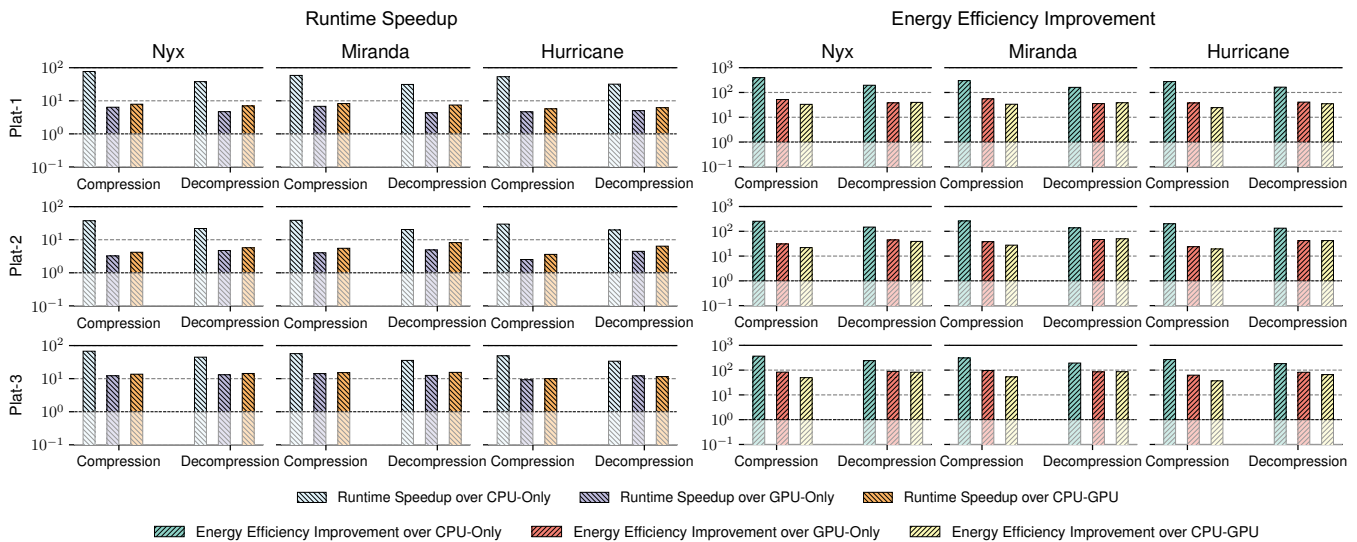
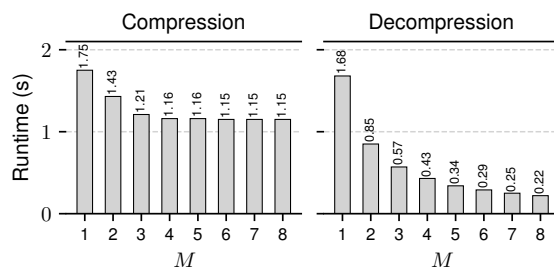
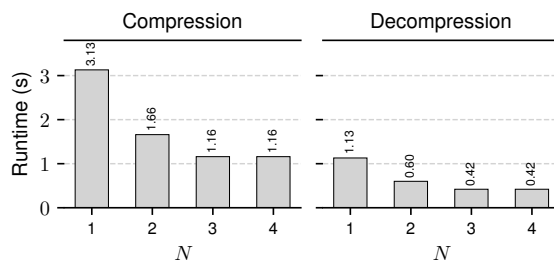


Figure 9: Evaluation of runtime speedup and energy efficiency.



(a) Data-size scalability. Compression and decompression runtime on the Nyx dataset with M scaled from 1 to 8.



(b) Workload scalability. Compression and decompression runtime for two Nyx, one Miranda, and one Hurricane datasets with N scaled from 1 to 4.

Figure 10: Scalability analysis of the proposed FLARE.

overall speedup depends on workload distribution and system bottlenecks—particularly those introduced by the neural network or dataset-specific characteristics.

Data movement reduction. To quantify the impact of the proposed architecture on data movement, we analyze internal data transfers within a single FLARE Computing Core, focusing on the Prediction Engine, Neural Engine, and Codec Engine, which are identified as the primary contributors to data movement during

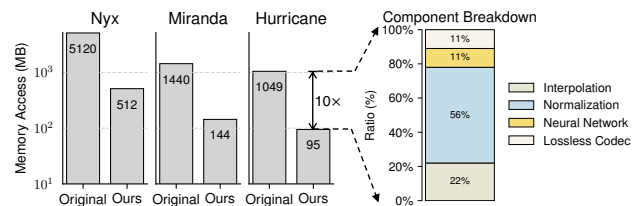


Figure 11: Off-chip data movement reduction of FLARE.

both compression and decompression. The look-ahead processing strategy in the Prediction Engine enables early reuse of intermediate results stored in on-chip SRAM, significantly reducing redundant data transfers. Additionally, the systolic array architecture promotes localized data reuse by maintaining data within processing elements, thereby minimizing costly off-chip memory accesses. Furthermore, the hybrid dataflow enhances efficiency by enabling pipelined and parallel execution across engines, effectively eliminating unnecessary off-chip communication between modules. The operator fusion strategy further contributes by integrating slice-wise normalization directly into the convolution kernel, eliminating separate memory accesses for normalization and convolution stages. Collectively, these architectural features streamline on-chip data access and substantially reduce overall data movement.

As shown in Figure 11, the proposed architecture achieves up to a 10 \times reduction¹ in data movement across three scientific datasets. Among the total reduction achieved, the largest contribution comes from normalization (56%), followed by prediction (22%), neural network operations (11%), and lossless codec (11%). These results underscore the effectiveness of the proposed design in minimizing

¹The data access during neural network training and inference is optimized via TimeLoop and excluded from this analysis. Thus, the data access pattern is identical in both compression and decompression procedures.

data movement and enhancing performance across diverse compression and decompression workloads.

5 Conclusion

This paper presents FLARE, a dataflow-aware and scalable hardware architecture for accelerating neural-hybrid scientific lossy compression. We introduce a look-ahead computation order that reduces SRAM usage and improves pipeline throughput. A slice-wise normalization method is further fused into convolution operations to minimize bubble overhead and reduce data movement. Then, we propose a scalable FLARE Computing Core, which enables efficient hybrid execution and scales effectively with both dataset size and workload volume. To our knowledge, this is the first customized design for lossy compression of scientific data that simultaneously addresses dataflow efficiency and architectural scalability. Experimental results show significant performance improvements over state-of-the-art baselines in terms of runtime latency and energy efficiency.

References

- [1] Ann S Almgren, John B Bell, Mike J Lijewski, Zarija Lukić, and Ethan Van Andel. 2013. Nyx: A massively parallel amr code for computational cosmology. *The Astrophysical Journal* 765, 1 (2013), 39.
- [2] Babak Behzad, Surendra Byna, Prabhat, and Marc Snir. 2019. Optimizing i/o performance of hpc applications with autotuning. *ACM Transactions on Parallel Computing (TOPC)* 5, 4 (2019), 1–27.
- [3] Franck Cappelto, Allison Baker, Ebru Bozda, Martin Burtscher, Kyle Chard, Sheng Di, Paul Christopher O Grady, Peng Jiang, Shaomeng Li, Erik Lindahl, et al. 2025. Lossy Compression of Scientific Data: Applications Constrains and Requirements. *arXiv preprint arXiv:2503.20031* (2025).
- [4] Sudheer Chunduri, Taylor Groves, Peter Mendygral, Brian Austin, Jacob Balma, Krishna Kandalla, Kalyan Kumaran, Glenn Lockwood, Scott Parker, Steven Warren, et al. 2019. Gpnet: Designing a benchmark suite for inducing and measuring contention in hpc networks. In *Proceedings of the International Conference for High Performance Computing, Networking, Storage and Analysis*. 1–33.
- [5] P. Deutsch. 1996. RFC1952: GZIP file format specification version 4.3.
- [6] Sheng Di and Franck Cappelto. 2016. Fast Error-Bounded Lossy HPC Data Compression with SZ. In *2016 IEEE International Parallel and Distributed Processing Symposium (IPDPS)*. IEEE Computer Society, Los Alamitos, CA, USA, 730–739. doi:10.1109/IPDPS.2016.11
- [7] Sheng Di, Jinyang Liu, Kai Zhao, Xin Liang, Robert Underwood, Zhaorui Zhang, Milan Shah, Yafan Huang, Jiajun Huang, Xiaodong Yu, et al. 2024. A survey on error-bounded lossy compression for scientific datasets. *arXiv preprint arXiv:2404.02840* (2024).
- [8] Jean-loup Gailly and Mark Adler. 2004. zlib Compression Library. <http://www.dspace.cam.ac.uk/handle/1810/3486> Accessed: 2025-01-08.
- [9] Kurt Hornik, Maxwell Stinchcombe, and Halbert White. 1989. Multilayer feed-forward networks are universal approximators. *Neural networks* 2, 5 (1989), 359–366.
- [10] Yafan Huang, Sheng Di, Guanpeng Li, and Franck Cappelto. 2024. cuSZp2: A GPU Lossy Compressor with Extreme Throughput and Optimized Compression Ratio. In *SC24: International Conference for High Performance Computing, Networking, Storage and Analysis*. IEEE, 1–18.
- [11] Wenqi Jia, Sian Jin, Jinzhen Wang, Wei Niu, Dingwen Tao, and Miao Yin. 2024. GWLZ: A Group-wise Learning-based Lossy Compression Framework for Scientific Data. In *Proceedings of the 14th Workshop on AI and Scientific Computing at Scale Using Flexible Computing Infrastructures (Pisa, Italy) (Flex-Science'24)*. Association for Computing Machinery, New York, NY, USA, 34–41. doi:10.1145/3659995.3660041
- [12] Wenqi Jia, Youyuan Liu, Zhewen Hu, Jinzhen Wang, Boyuan Zhang, Wei Niu, Junzhou Huang, Stavros Kalafatis, Sian Jin, and Miao Yin. 2024. NeurLZ: On Enhancing Lossy Compression Performance based on Error-Controlled Neural Learning for Scientific Data. *arXiv preprint arXiv:2409.05785* (2024).
- [13] Nnadikwe Johnson. 2023. Exploring Cutting-Edge Application of Computational Fluid Dynamic in Enhancing and Innovation within the Oil and Gas Sector. (12 2023). doi:10.20944/preprints202312.1113.v1
- [14] Yao Kang, Xin Wang, and Zhiling Lan. 2022. Study of workload interference with intelligent routing on dragonfly. In *SC22: International Conference for High Performance Computing, Networking, Storage and Analysis*. IEEE, 1–14.
- [15] Sunggon Kim, Alex Sim, Kesheng Wu, Suren Byna, and Yongseok Son. 2023. Design and implementation of I/O performance prediction scheme on HPC systems through large-scale log analysis. *Journal of Big Data* 10, 1 (2023), 65.
- [16] Sriram Lakshminarasimhan, Neil Shah, Stephane Ethier, Seung-Hoe Ku, Choong-Seock Chang, Scott Klasky, Rob Latham, Rob Ross, and Nagiza F Samatova. 2013. ISABELA for effective in situ compression of scientific data. *Concurrency and Computation: Practice and Experience* 25, 4 (2013), 524–540.
- [17] Xiao Li, Jaemoon Lee, Anand Rangarajan, and Sanjay Ranka. 2024. Attention Based Machine Learning Methods for Data Reduction with Guaranteed Error Bounds. arXiv:2409.05357 [cs.LG] <https://arxiv.org/abs/2409.05357>
- [18] Xin Liang, Sheng Di, Sihuan Li, Dingwen Tao, Bogdan Nicolae, Zizhong Chen, and Franck Cappelto. 2019. Significantly improving lossy compression quality based on an optimized hybrid prediction model. In *Proceedings of the International Conference for High Performance Computing, Networking, Storage and Analysis (Denver, Colorado) (SC '19)*. Association for Computing Machinery, New York, NY, USA, Article 33, 26 pages. doi:10.1145/3295500.3356193
- [19] Xin Liang, Kai Zhao, Sheng Di, Sihuan Li, Robert Underwood, Ali M Gok, Jiannan Tian, Junjing Deng, Jon C Calhoun, Dingwen Tao, et al. 2022. Sz3: A modular framework for composing prediction-based error-bounded lossy compressors. *IEEE Transactions on Big Data* 9, 2 (2022), 485–498.
- [20] Peter Lindstrom. 2014. Fixed-rate compressed floating-point arrays. *IEEE transactions on visualization and computer graphics* 20, 12 (2014), 2674–2683.
- [21] Peter Lindstrom and Martin Isenburt. 2006. Fast and efficient compression of floating-point data. *IEEE transactions on visualization and computer graphics* 12, 5 (2006), 1245–1250.
- [22] Jinyang Liu, Sheng Di, Sian Jin, Kai Zhao, Xin Liang, Zizhong Chen, and Franck Cappelto. 2023. Scientific error-bounded lossy compression with super-resolution neural networks. In *2023 IEEE International Conference on Big Data (BigData)*. IEEE, 229–236.
- [23] Jinyang Liu, Sheng Di, Kai Zhao, Sian Jin, Dingwen Tao, Xin Liang, Zizhong Chen, and Franck Cappelto. 2021. Exploring autoencoder-based error-bounded compression for scientific data. In *2021 IEEE International Conference on Cluster Computing (CLUSTER)*. IEEE, 294–306.
- [24] Jinyang Liu, Sheng Di, Kai Zhao, Xin Liang, Zizhong Chen, and Franck Cappelto. 2022. Dynamic Quality Metric Oriented Error Bounded Lossy Compression for Scientific Datasets. In *SC22: International Conference for High Performance Computing, Networking, Storage and Analysis*. IEEE Computer Society, Los Alamitos, CA, USA, 1–15. doi:10.1109/SC41404.2022.00067
- [25] Jinyang Liu, Jiannan Tian, Shixun Wu, Sheng Di, Boyuan Zhang, Robert Underwood, Yafan Huang, Jiajun Huang, Kai Zhao, Guanpeng Li, et al. 2024. CUSZ-i: High-Ratio Scientific Lossy Compression on GPUs with Optimized Multi-Level Interpolation. In *SC24: International Conference for High Performance Computing, Networking, Storage and Analysis*. IEEE, 1–15.
- [26] Youyuan Liu, Wenqi Jia, Taolue Yang, Miao Yin, and Sian Jin. 2024. Enhancing Lossy Compression Through Cross-Field Information for Scientific Applications. In *SC24-W: Workshops of the International Conference for High Performance Computing, Networking, Storage and Analysis*. 300–308. doi:10.1109/SCW63240.2024.00046
- [27] Zarija Lukić, Casey W Stark, Peter Nugent, Martin White, Avery A Meiksin, and Ann Almgren. 2015. The Lyman α forest in optically thin hydrodynamical simulations. *Monthly Notices of the Royal Astronomical Society* 446, 4 (2015), 3697–3724.
- [28] John D. McCalpin. 2023. Bandwidth Limits in the Intel Xeon Max (Sapphire Rapids with HBM) Processors. In *High Performance Computing*, Amanda Bienz, Michèle Weiland, Marc Baboulin, and Carola Kruse (Eds.). Springer Nature Switzerland, Cham, 403–413.
- [29] Gerald A Meehl, George J Boer, Curt Covey, Mojib Latif, and Ronald J Stouffer. 2000. The coupled model intercomparison project (CMIP). *Bulletin of the American Meteorological Society* 81, 2 (2000), 313–318.
- [30] Jose Oñorbe, FB Davies, Z Lukić, JF Hennawi, and D Sorini. 2019. Inhomogeneous reionization models in cosmological hydrodynamical simulations. *Monthly Notices of the Royal Astronomical Society* 486, 3 (2019), 4075–4097.
- [31] Angshuman Parashar, Priyanka Raina, Yakun Sophia Shao, Yu-Hsin Chen, Victor A Ying, Anurag Mukkara, Rangharajan Venkatesan, Brucec Khailany, Stephen W Keckler, and Joel Emer. 2019. Timeloop: A systematic approach to dnn accelerator evaluation. In *2019 IEEE international symposium on performance analysis of systems and software (ISPASS)*. IEEE, 304–315.
- [32] Arnab K Paul, Olaf Falaland, Adam Moody, Elsa Gonsiorowski, Kathryn Mohror, and Ali R Butt. 2020. Understanding hpc application i/o behavior using system level statistics. In *2020 IEEE 27th International Conference on High Performance Computing, Data, and Analytics (HiPC)*. IEEE, 202–211.
- [33] Reinaldo R Rosa. 2020. Data Science Strategies for Multimessenger Astronomy. *Anais da Academia Brasileira de Ciências* 93 (2020), e20200861.
- [34] Jean Sexton, Zarija Lukic, Ann Almgren, Chris Daley, Brian Friesen, Andrew Myers, and Weiqun Zhang. 2021. Nyx: A massively parallel amr code for computational cosmology. *The Journal of Open Source Software* 6, 63 (2021), 3068.

- [35] Dingwen Tao, Sheng Di, Zizhong Chen, and Franck Cappelto. 2017. Significantly Improving Lossy Compression for Scientific Data Sets Based on Multidimensional Prediction and Error-Controlled Quantization . In *2017 IEEE International Parallel and Distributed Processing Symposium (IPDPS)*. IEEE Computer Society, Los Alamitos, CA, USA, 1129–1139. doi:10.1109/IPDPS.2017.115
- [36] Dingwen Tao, Sheng Di, Xin Liang, Zizhong Chen, and Franck Cappelto. 2019. Optimizing lossy compression rate-distortion from automatic online selection between SZ and ZFP. *IEEE Transactions on Parallel and Distributed Systems* 30, 8 (2019), 1857–1871.
- [37] Jiannan Tian, Sheng Di, Kai Zhao, Cody Rivera, Megan Hickman Fulp, Robert Underwood, Sian Jin, Xin Liang, Jon Calhoun, Dingwen Tao, et al. 2020. Cusz: An efficient gpu-based error-bounded lossy compression framework for scientific data. In *Proceedings of the ACM International Conference on Parallel Architectures and Compilation Techniques*. 3–15.
- [38] Kai Zhao, Sheng Di, Maxim Dmitriev, Thierry-Laurent D. Tonellot, Zizhong Chen, and Franck Cappelto. 2021. Optimizing Error-Bounded Lossy Compression for Scientific Data by Dynamic Spline Interpolation . In *2021 IEEE 37th International Conference on Data Engineering (ICDE)*. IEEE Computer Society, Los Alamitos, CA, USA, 1643–1654. doi:10.1109/ICDE51399.2021.00145
- [39] Kai Zhao, Sheng Di, Xin Lian, Sihuan Li, Dingwen Tao, Julie Bessac, Zizhong Chen, and Franck Cappelto. 2020. SDRBench: Scientific Data Reduction Benchmark for Lossy Compressors . In *2020 IEEE International Conference on Big Data (Big Data)*. IEEE Computer Society, Los Alamitos, CA, USA, 2716–2724. doi:10.1109/BigData50022.2020.9378449
- [40] Jacob Ziv and Abraham Lempel. 1977. A universal algorithm for sequential data compression. *IEEE Transactions on information theory* 23, 3 (1977), 337–343.